Journal of Cellular Biochemistry 82:246–259 (2001)

Cloning and Characterization of Human Syndecan-3

Christine Berndt, Ricardo P. Casaroli-Marano, Senén Vilaró, and Manuel Reina*

Department of Cell Biology, University of Barcelona, Diagonal 645, 08028 Barcelona, Spain

Abstract Syndecans are cell-surface heparan sulfate proteoglycans, which perform a variety of functions in the cell. Most important, they are co-receptors for growth factors and mediate cell–cell and cell–matrix interactions. Four syndecans (syndecan 1–4) have been described in different species. The aim of this work was the cloning and characterization of human syndecan-3. The human syndecan-3 sequence has high homology to the rat and mouse sequences, with the exception of the 5′-region. Syndecan-3 mRNA is mostly expressed in the nervous system, the adrenal gland, and the spleen. When different cell lines were transiently transfected with full-length syndecan-3 cDNA, it was localized to the membrane and induced the formation of long filopodia-like structures, microspikes, and varicosities. Consequently, the actin cytoskeleton was re-organized, since actin staining was mostly found in the cellular extensions and at the cell periphery, co-localizing with the syndecan-3 staining. The development of the phenotype depended on the presence of sugar chains, as transfected glycosaminoglycan-deficient Chinese hamster ovary (CHO) 745 cells did not show these structural changes, nor did transfected CHO K1 cells in the presence of heparin. The similarity of the cloned DNA sequence with that of other mammalian species and the high expression in the nervous system led us to the assumption that human syndecan-3 could perform comparable functions to those described for syndecan-3 in rat and mouse. Additionally, transient transfection experiments suggest a role of human syndecan-3 in the organization of cell shape by affecting the actin cytoskeleton, possibly by transferring signals from the cell surface in a sugar-dependent mechanism. J. Cell. Biochem. 82: 246–259, 2001.

Key words: syndecan-3; actin cytoskeleton; filopodia

Mammalian cells are endowed with a variety of cell-surface receptors, which mediate cell–matrix and cell–cell adhesion. The most prominent members of these families are the integrins [Howe et al., 1998] and cadherins [Takeichi, 1991], but many groups have recently focused on the syndecans. Syndecans are heparan sulfate proteoglycans (HSPGs) belonging to the family of type I transmembrane proteins [Bernfield et al., 1992; Carey, 1997a; Woods and Couchman, 1998; Zimmermann and David, 1999]. Four syndecans have been described so far: syndecan-1, -2 (fibroglycan), -3 (N-syndecan), and -4 (ryudocan, amphiglycan), which are expressed by four different genes in a tissue-specific and developmentally regulated manner [Kim et al., 1994]. Syndecan-1 is most abundant in epithelial tissue, syndecan-2 is mainly found in fibroblasts, syndecan-3 is predominant in the central nervous system (CNS), while syndecan-4 is expressed by multiple cell types [Zimmermann and David, 1999].

The main function of the syndecans is unknown. They have been described as co-receptors for growth factors (e.g., basic fibroblast growth factor, (bFGF)), low affinity receptors for enzymes (such as lipoprotein lipase, LPL), mediators of cell–cell and cell–matrix interactions (co-operating with integrins), co-receptors

Abbreviations used: BFGF, basic fibroblast growth factor; bp, base pair; CHO, chinese hamster ovary; CLSM, confocal laser scanning microscopy; CNS, central nervous system; DEAE-dextran, diethylaminoethyl-dextran; ECM, extracellular matrix; ERM proteins, Ezrin-Radixin-Moesin proteins; GAG, glycosaminoglycan; GFP, green fluorescent protein; HB-GAM, heparin binding growth-associated molecule; HSPGs, heparan sulfate proteoglycans; LPL, lipoprotein lipase; LSC, laser scanning cytometer; LTP, long term potentiation, WASP, Wiskott-Aldrich syndrome protein; ORF, open reading frame.

The nucleotide sequence reported in this paper has been submitted to the Genbank/EMBL Data Bank with registration number AF248634.

Grant sponsor: European Commission; Grant number: BMH4-CT98-5142; Grant sponsor: Studienstiftung des Deutschen Volkes; Fundació Marató TV3.

*Correspondence to: Dr. Manuel Reina, Department of Cell Biology, School of Biology, University of Barcelona, Avda. Diagonal 645, E-08028-Barcelona, Spain.
E-mail: mreina@porthos.bio.ub.es

Received 14 July 2000; Accepted 10 January 2001

for proteases and their inhibitors, and receptors for viruses [Carey, 1997a].

All syndecans have a common structure. They possess a large extracellular domain with a signal peptide and varying amounts of glycosaminoglycan (GAG) attachment sites, a single transmembrane domain and a very short (28–34 amino acids) cytoplasmic domain. They differ in their extracellular domains, but show high homology ($>50\%$) in the transmembrane and C-terminal domains. The latter contains four tyrosine residues that are 100% conserved in all known syndecans and might serve as putative phosphorylation sites. The last four amino acids of the cytoplasmic tail (EFYA), also identical in all syndecans, represent the binding sequence for PDZ domain-containing proteins.

Syndecan-3, also called N-syndecan due to its abundance in the nervous system was first cloned in rat from a Schwann cell and a rat-brain library [Carey et al., 1992, 1997b]. Its expression strongly correlates with the differentiation of oligodendrocytes and myelination in the central and peripheral nervous systems [Carey, 1996]. Syndecan-3 also contributes to cartilage [Gould et al., 1992] and skeletal muscle differentiation [Fuentealba et al., 1999].

Syndecan-3 binds to bFGF during nervous tissue development [Chernousov and Carey, 1993]. It promotes attachment and spreading of Schwann cells [Chernousov et al., 1996] by binding to p200, a heparin-binding glycoprotein secreted by Schwann cells. Syndecan-3 is also receptor for the cell-surface and extracellular matrix-(ECM)-associated molecule HB-GAM (heparin binding growth-associated molecule) in brain neurons [Raulo et al., 1994; Kinnunen et al., 1996]. This binding leads to neurite outgrowth in which the cortactin-src kinase-signaling pathway is involved [Kinnunen et al., 1998]. Nolo et al. [1995] showed that syndecan-3 and HB-GAM are co-expressed in the developing rat brain. Finally, syndecan-3 has a crucial role in synaptic plasticity by regulating long term potentiation (LTP) in the CA1 region of the hippocampus [Lauri et al., 1998, 1999].

Since all these studies were performed with rat, mouse, or chicken syndecan-3, we focused our interest on the cloning of the human syndecan-3 cDNA. Interestingly, although the human protein sequence was similar to that of rodents, in the N-terminal region, where the hypothetical signal peptide is located, we observed 17 distinct amino acids. We found that the main expression sites of the syndecan-3 mRNA are the nervous system, the adrenal glands, and the spleen. We showed that the transient expression of syndecan-3 in different cell types led to the induction of long, filopodia-like structures and microspikes, and to the reorganization of the actin cytoskeleton, which was dependent on the presence of GAG chains in the syndecan-3 protein.

METHODS

Library and Screening

Human syndecan-3 cDNA was isolated by double screening of a human fetal brain λZAP II library. *Escherichia coli* cells, strain XL1-Blue, were infected with the bacteriophages and plated on LB agar plates with tetracycline. Filter lifts were prepared from 50,000 recombinant plaques onto nitrocellulose filters (0.45 μm; Schleicher + Schull, Germany) and hybridized to a ^{32}P-labeled oligonucleotide (Random Primed Labeling Kit, Boehringer Mannheim, Germany), corresponding to the ectodomain of syndecan-3 (fragment EcoRI-BamHI of pMB284 corresponding to about 700 bp of the ectodomain, a generous gift from Dr. M. Bernfield). The filters were moistened in $6 \times$ SSC and pre-hybridized for 2 h with the following solution: $5 \times$ SSC; $5 \times$ Denhardt's solution; 20 mM PO_4^-; 50% formamid; 0.5% SDS and 0.15 mg/ml single-strand salmon sperm DNA. The filters were hybridized overnight at 42°C in the solution described above with 1.4% dextran-sulfate and the radioactive labeled probe. ($1 \times$ SSC = 0.15 M NaCl; 0.015 M sodium citrate; pH 7.2). The filters were washed for 10 min at room temperature and 2×30 min at 65°C in $0.5 \times$ SSC and 0.5% SDS, then 2×30 min at 65°C in $0.2 \times$ SSC and 0.5% SDS, and a Kodak X-OMAT UV film was exposed to the filters at −80°C with intensifying screens. 27 positive clones were found.

Bacteriophages were recombined with a helper phage (ExAssist helper phage, Stratagene, La Jolla) to integrate the different clones into doublesstrand pBluescript II KS±phagemid. *E. coli* cells, strain SORL, were transfected with the different phagemids. DNA inserts were excised from pBluescript II KS±by digestion with *EcoR*I (Biolabs, New England) and subcloned into the *EcoR*I site of the plasmid pGEM3zf (+) (Promega, Madison, WT). Sequencing (Thermo Sequenase I and II Dye

Terminating Cycle Sequencing Kit, Amersham Life Science, Cleveland) showed that none of these overlapping clones contained the full-length cDNA. Therefore we replaced the 5′-end of the cDNA corresponding to the fragment from the *EcoR*I site to the *Sac*I site (*Sac*I: Pharmacia, Uppsala, Sweden) of clone #42, which contains the full 3′-coding region to the stop-codon, with the corresponding region of clone #40, which contains the ATG-start codon. The resulting plasmid was named *Ce5*.

Expression Constructs

For expression in mammalian cells, the full-length construct *Ce5* was cut with *EcoR*I/*Hind*III (*Hind*III: Pharmacia, Uppsala, Sweden) and subcloned into the corresponding restriction sites of pRK5. Two different constructs were prepared containing the Green Fluorescent Protein (GFP) as tag. To obtain the full-length syndecan-3 sequence at the N-terminal end of the fusion protein (*S3GFP*), PCR was performed on *Ce5* to introduce an *EcoR*I and a *BamH*I restriction site (Eco-synd3: 5′-TAC GAC TCA CTA TAG GGC GAA TTC and Synd3-NS-BamHI: 5′-GAT CGG ATC CGC TCC ACA AGG CAT AGA ACT CC). This fragment was subcloned into the pEGFP-N3 vector (Clontech, Palo Alto, California). Errors produced by PCR were observed in the 5′-region of our sequence. As there was no way to improve the PCR due to a GC-rich region at the 5′-end, we performed a ligation with three components: Clone #40 was cut with *EcoR*I-*Sac*I, *S3GFP* was cut with *Sac*I-*BamH*I and both fragments were mixed with the *EcoR*I-*BamH*I cut pEGFP-N3 vector and ligated to obtain the correct *S3GFP*. Sequencing confirmed the correct ligation of the three components.

GFPS3, carrying the full-length syndecan-3 sequence in the C-terminal domain of the fusion protein, was engineered by cutting *Ce5* with *Hind*III, by treating the linearized plasmid with Klenow Polymerase (Boehringer Mannheim, Mannheim, Germany) and then by cutting with *EcoR*I. This fragment was subcloned into the GFP-C2 vector (Clontech, Palo Alto, California) digested with *Sma*I (Promega, Madison) and *EcoR*I. All primers were purchased from Boehringer Mannheim, Mannheim, Germany.

RNA Dot Blot

A poly A RNA dot blot from human tissues and cell lines (Clontech, Palo Alto, California) was incubated with a radioactive labeled ^{32}P-labeled probe corresponding to the ectodomain of syndecan-3 (fragment *EcoR*I-*BamH*I of pMB284). The manufacture's instructions were followed. Densitometry measurements were performed by using a phosphoimager (Biorad, Germany). Results were analyzed with Molecular Analyst software (Biorad, Germany).

Cell Culture and Transfection Experiments

COS-1 cells were cultured in Dulbecco's Modified Eagle's Medium with 4.5 g/l of glucose, supplemented with 10% FCS (Whittaker, Indianapolis, IN), antibiotics and 2 mM glutamine (Sigma, Deisenhofen, Germany) at 37°C, 5% CO_2 and 90% of humidity. 3T3 cells were cultured in the same conditions except for glucose concentration (1 g/l). CHO K1 and CHO 745 cells were cultured in Ham's F10 medium (Whittaker, Indianapolis, IN), supplemented with 10% FCS and containing antibiotics and glutamine as described above. COS-1 cells (40–50% confluence) were transfected 20 h after plating with the diethylaminoethyl-(DEAE)-dextran/chloroquine method (25 ng DNA/cm^2). Transfection experiments with Swiss 3T3 cells (30–40% confluence) were performed 20 h after plating by using the Superfect Transfection Agent (Qiagen, Germany) and a DNA concentration of 170 ng/cm^2. CHO K1 and CHO 745 cells were plated to a final density of 50–70% and transfected after 20 h with the aid of the Superfect Agent (DNA concentration: 70 ng/cm^2). All cell lines were plated on coverslips. The vectors used in the experiments were the full-length syndecan-3 in pRK5, *S3GFP* and *GFPS3*.

Immunofluorescence Analysis

Cells grown on coverslips were rinsed in 100 mM PBS and fixed with 3% paraformaldehyde (Merck, Darmstadt, Germany), 2% sucrose (Sigma) in 100 mM phosphate buffer, pH 7.4, for 20–45 min at room temperature. Cells were washed three times in 10 mM PBS and 20 mM glycine (Sigma). Blocking was performed for 10 min with PBS and 20 mM glycine in the presence of 1% bovine serum albumin (BSA, Sigma) at room temperature. For syndecan-3 detection, coverslips were incubated with polyclonal rabbit anti-syndecan-3 antibody (a generous gift from Dr. M. Bernfield), diluted 1:200 in the blocking solution, for 1 h at 37°C. To

visualize rabbit antibodies, FITC-conjugated swine anti-rabbit (dilution 1:50) was used (DAKO, Denmark). For co-localization of syndecan-3 with actin, coverslips were then further incubated with TRITC-conjugated phalloidin (1:2000; Sigma) in blocking solution containing 0.1% Triton X-100 for 10 min (Sigma).

CHO K1 and CHO 745 cells were transfected as described above and analyzed 48 h after transfection. Analysis was performed using a fluorescent microscope (Axioskop, Zeiss, Germany), with 63X/1,4 oil DIC objective (Zeiss, Germany). All anti-syndecan-3 labeled cells were counted, and the proportion of cells showing the typical syndecan-3 phenotype was evaluated in respect to the total transfected, syndecan-3 positive population. Collapsed cells were not taken into consideration, even if they sometimes showed very strong staining. The results were obtained from three independent experiments. The total number of cells counted was 749 CHO K1 and 183 CHO 745 cells.

Heparin Treatment

After transfection, CHO K1 cells were maintained for 48 h in presence of 10 U/ml heparin (Sigma). As a control, a culture dish was incubated in the same conditions but without heparin treatment. Cells were analyzed as described above. Three independent experiments were performed. The number of coverslips analyzed was six in the control and 14 in the heparin treated experiment.

Confocal Microscopy and Electron Microscopy

Confocal laser scanning microscopy (CLSM) was performed with a Leica TCS 4D (Leica Lasertechnik GmbH, Heidelberg, Germany), adapted to an inverted microscope (Leitz DMIRB). To obtain images, the 63X (NA 1.3, Ph3, oil) Leitz Plan-Apochromatic objective was used. FITC and TRITC were excited by sequential excitation at 488- and 568-nm lines of a krypton-argon laser. Three-dimensional projections were made from horizontal sections. Each image represents the average of eight line scans at the standard scan rate, but some structural details were collected with slow scan rate. Scanning electron microscopy was performed as described before [Granés et al., 1999].

RESULTS

Human Syndecan-3 cDNA and Protein Sequences

Human syndecan-3 cDNA was isolated by screening a human λ ZAP library with a ^{32}P-labeled probe corresponding to a fragment of the ectodomain of the human syndecan-3 sequence. 27 overlapping clones were obtained, but none of them contained the entire cDNA sequence. Nevertheless, we obtained full-length sequence by combining the 5′-region of one clone (#40) with the 3′-region of another (#42) by enzymatic restrictions and ligation. The resulting vector (named *Ce5*) was subcloned and sequenced.

The DNA sequence revealed an open reading frame (ORF) of 1329 bp, predicting a polypeptide of 443 amino acids (Fig. 1A). The protein sequence can be divided into three different structural domains (Fig. 1B): a large extracellular domain, followed by a single glycine rich transmembrane domain and a short cytoplasmic tail (34 amino acids). The extracellular domain bears a proline-rich spacer and eight putative GAG attachment sites (represented by the dipeptide repeat serine and glycine). These attachment sites are arranged in two clusters, located distal (five dipeptide repeats) and proximal (three dipeptide repeats) to the plasma membrane. Next to the transmembrane region, a dibasic repeat is found. The cytoplasmic tail contains three characteristic regions of syndecans: two constant (C_1- and C_2-) regions, separated by a variable (V-) region. In these regions four 100% conserved tyrosine residues are located. The second constant region consists of four amino acids (EFYA), the motif interacting with PDZ domain-containing proteins.

The amino acid sequence of the human syndecan-3 showed high homology (62% with chicken and 84% with rat), reaching 100% in the transmembrane and cytoplasmic domain compared with rodents. Only amino acids 7–23 from all our analyzed clones were different (Fig. 2). This stretch, lying in the region of the hypothetical signal peptide, is characterized by an accumulation of small, neutral amino acids (82%). Thus, 9/17 and 5/17 are glycine and alanine residues, respectively. No identical sequence was found in a data base search.

Expression Studies of Human Syndecan-3 mRNA

To examine the expression of human syndecan-3 mRNA, the oligonucleotide probe used in the screening process was labeled with ^{32}P and

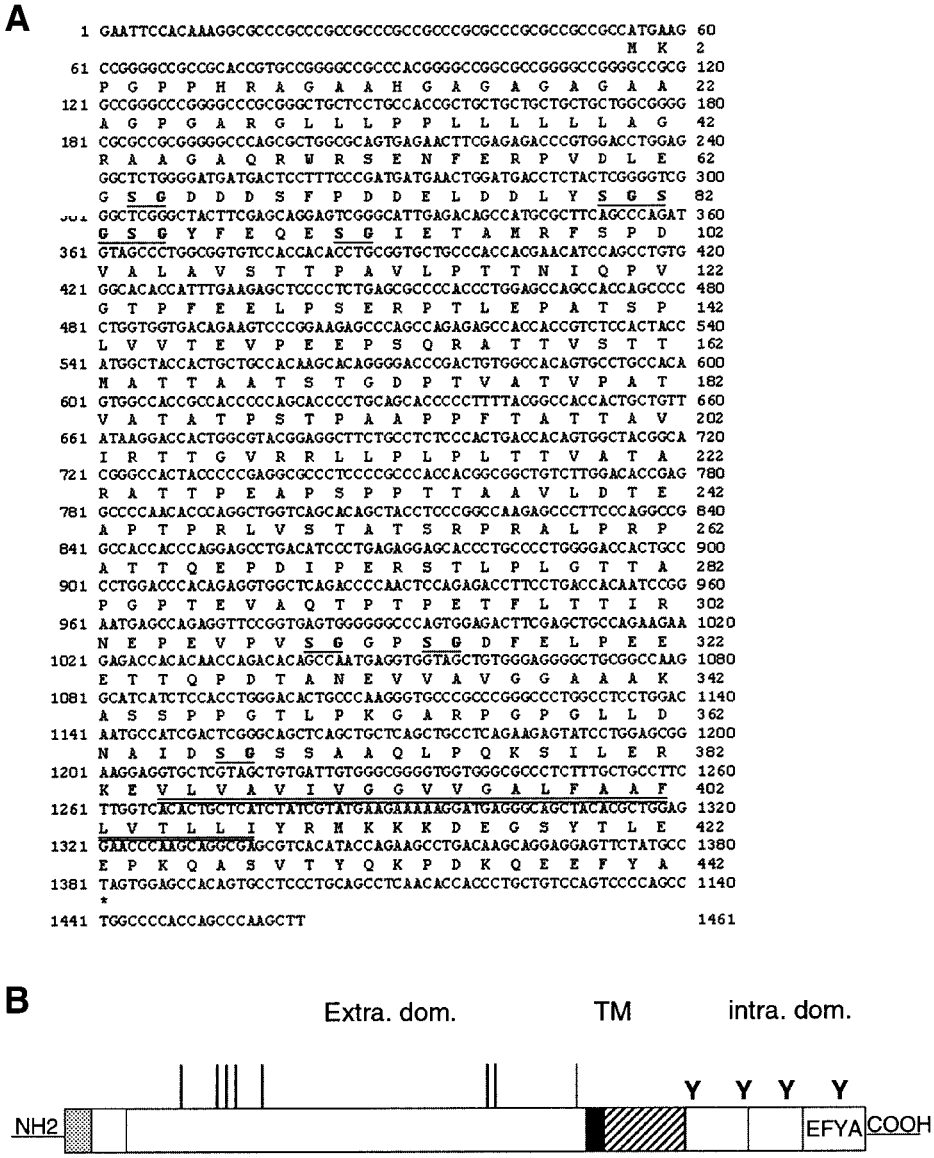

Fig. 1. Organization of human syndecan-3. **A:** cDNA and aligned protein sequence of the human syndecan-3 gene. Putative GAG attachment sites (serine and glycine) are underlined once. Transmembrane sequence is double underlined, the stop codon is indicated by an asterisk. **B:** Schematic representation of human syndecan-3 protein structure. The gray box represents the human specific syndecan-3 sequence, vertical lines indicate the putative GAG attachment sites, the black box marks the dibasic repeat and the hatched box the transmembrane region. Bold "Y's" are symbolizing the tyrosine residues in the C-terminal. The final amino acid sequence EFYA is the interacting motif with intracellular PDZ proteins.

used to perform a RNA dot blot analysis of 76 human poly A^+ RNA's (from various tissues and cell lines) and 8 control RNA's. As shown in Figure 3A, syndecan-3 was mostly expressed in the brain (adult and fetal), the adrenal gland, and the spleen. In the nervous system strong expression was found in almost all regions examined, except for the pituitary gland. Very strong labeling was detected in the temporal lobe (highest levels), in the corpus callosum and the spinal cord (Fig. 3B). In the gastrointestinal system, syndecan-3 RNA was mainly found in the stomach, transverse colon, in the descending colon, the duodenum, and in the rectum, while in the heart expression was predominantly found in the aorta (data not shown). In fetal tissues, strong signals were obtained with the RNA from fetal brain and spleen. The only cell line from three leukemia, two lymphoma, one lung carcinoma, one adenocarcinoma cell

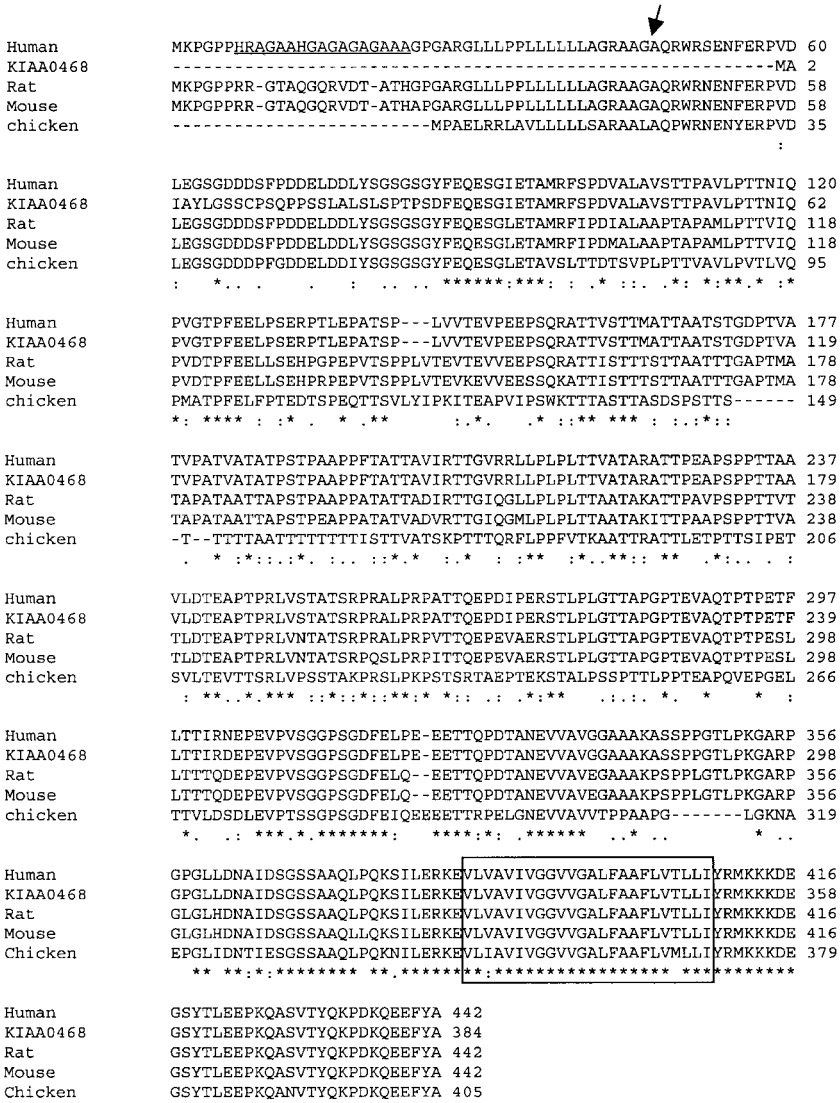

Fig. 2. Alignment of the human syndecan-3 protein with its rat, mouse, and chicken homologue. Although almost the whole human syndecan-3 sequence is very similar to that of mouse and rat, amino acid 7–23 (underlined) corresponding to a region inside the hypothetical signal peptide are striking different. "*" = identical or conserved residues in all sequences in the alignment; ":" = conserved substitutions; "." = semi-conserved substitutions. Transmembrane region is marked by a box, the end of the hypothetical signal peptide of human syndecan-3 by an arrow. KIAA0468 represents the sequence of a human clone from the database, which was not further characterized.

lines, and HeLa cells, that showed syndecan-3 expression, was the colorectal adenocarcinoma cell line SW480 (data not shown).

Phenotype of Cells Transiently Transfected With Syndecan-3

In order to study the function of the syndecan-3 protein, transient transfection experiments were performed in COS-1 cells (Fig. 4). Cells were transfected with the control vector (Fig. 4A) or with the full-length syndecan-3 sequence (Fig. 4B,C), fixed 48 h post-transfection and immunolabeled with polyclonal anti-syndecan-3 antibody (Fig. 4A–C). Analyzed by confocal microscopy, strong membrane staining was observed in the syndecan-3 transfected cells (Fig. 4B,C), while in the control experiments only a diffuse background staining on the whole cell surface was detected. This result indicates that syndecan-3 located to the membrane, since the antibody is directed against the ectodomain of the protein and the immunocytochemistry was performed in non-permeabilized cells. The expression of the full-length

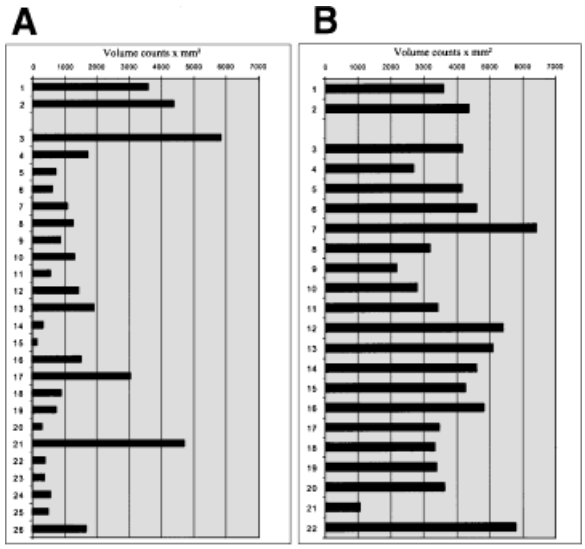

Fig. 3. Expression of syndecan-3 mRNA in different human tissues. For dot blot analysis, 76 human poly A^+ RNA's and 8 control RNA's arranged on a nylon membrane were incubated with a radioactively-labeled (^{32}P) syndecan-3 DNA oligonucleotide. The amount of radioactivity was determined using a phosphoimager. **A:** Expression of syndecan-3 in different human tissues (1 = whole brain, 2 = fetal brain, 3 = adrenal gland, 4 = bladder, 5 = bone marrow, 6 = kidney, 7 = liver, 8 = lung, 9 = lymph node, 10 = mammary gland, 11 = ovary, 12 = heart, 13 = stomach, 14 = pancreas, 15 = peripheral blood leukocyte, 16 = placenta, 17 = colon, transverse, 18 = prostata, 19 = salivary gland, 20 = skeletal muscle, 21 = spleen, 22 = testis, 23 = thymus, 24 = thyroid gland, 25 = trachea, 26 = uterus) and **(B)** in different regions from human brain (1 = whole brain, 2= fetal brain, 3 = cerebral cortex, 4 = frontal lobe, 5 = parietal lobe, 6 = occipital lobe, 7 = temporal lobe, 8 = paracentral gyrus of cerebral cortex, 9 = pons, 10 = cerebellum left, 11 = cerebellum right, 12 = corpus callosum, 13 = amygdala, 14 = caudate nucleus, 15 = hippocampus, 16 = medulla oblongata, 17 = putamen, 18 = substantia nigra, 19 = nucleus accumbens, 20 = thalamus, 21 = pituitary gland, 22 = spinal cord).

protein in COS-1 cells led to the induction of a large number of filopodia-like structures (arrows), some of which had varicosities on their tip (arrowheads). These effects were not seen in control (Fig. 4A). As well as the filopodia-like structures (>5 μm), transfected cells manifested abundant microspikes (<5 μm) on the surface of the cell membrane.

Surprisingly, COS-1 cells transfected with a construct in which GFP was fused to the C-terminal domain of syndecan-3 (*S3GFP*) also showed an altered phenotype (Fig. 4E, F; arrows indicate filopodia and arrowheads varicosities). This was unexpected, since GFP is a large molecule which should hinder interactions of the cytoplasmic tail with intracellular proteins. Nevertheless, the effect is not due to the presence of the GFP-molecule. Cells transfected with the vector bearing the GFP in the N-terminal domain of syndecan-3 (*GFPS3*; Fig. 4D) or with GFP alone showed the typical green color; but as GFP is a cytoplasmic protein, the fusion protein was not delivered to the membrane and also did not provoke the syndecan-3 phenotype. This indicates that the export of syndecan-3 to the membrane is a prerequisite for the formation of the filopodia-like structures. However, it must be said that the induction of the phenotype was not seen in all COS-1 cells after transfection with *S3GFP*. Therefore, it might be that the fusion protein had not yet reached or was not delivered correctly to the plasma membrane, even though GFP staining could be already seen. There were also some cells degenerating due to the abundance of GFP produced inside the cells (these cells often show a lot of vacuoles) which might also explain why these transfected cells do not produce long filopodia.

Syndecan-3 Co-Localizes With Re-Organized Actin Cytoskeleton

To verify that the effect observed was not unique to COS-1 cells, 3T3 (Fig. 5A–C) and CHO K1 (Fig. 5D–F) cells were transfected with the full-length construct and immunocytochemistry experiments were performed. In the transfected cells slightly different phenotypes were found, which were not specific to the original cell line and might originate in different levels of glycosylation. For every "phenotype" one representative example is shown. Some cells had an "ice-crystal"-like structure (Fig. 5A, C), often combined with a multitude of varicosities (arrowheads). The most dramatic effect was seen in CHO K1 cells, some of which had several hundred long projections (up to 50 μm) that originated in the cell body, sometimes without any ramifications (Fig. 5D) and sometimes displaying an abundance of varicosities (Fig. 5F; arrowheads).

The syndecan-3 protein co-localizes strongly with actin in all cell lines tested. The main sites of co-localization were the filopodia-like structures, the microspikes and cortical actin. 3T3 (Fig. 5A, B; arrows) and CHO K1 cells (Fig. 5D, E; arrows) are shown as examples. The distribution of the syndecan-3 protein was homogeneous inside the whole prolongation, while

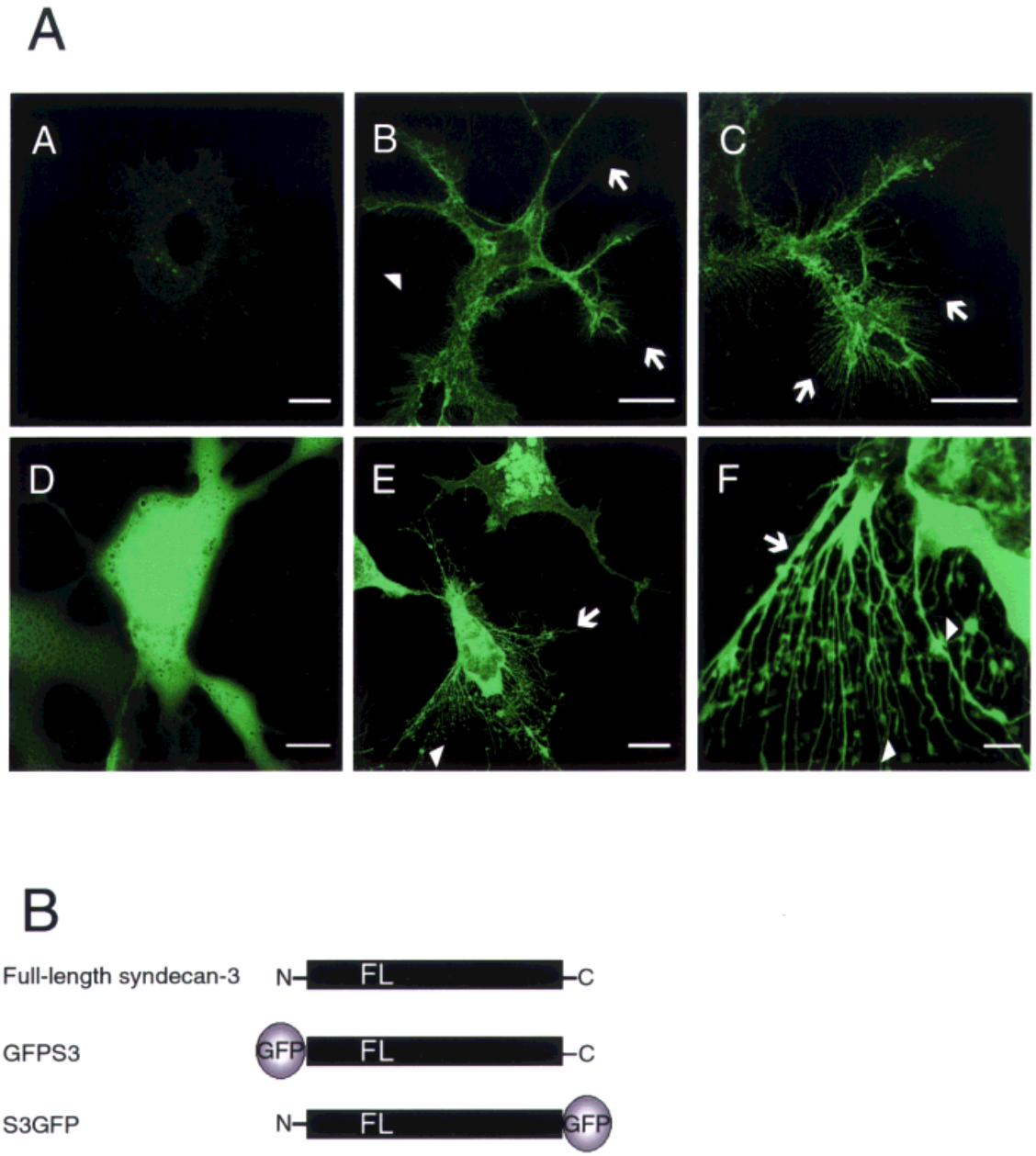

Fig. 4. Induction of filopodia-like structures, microspikes, and varicosities in COS-1. **(Panel A):** COS-1 cells were transiently transfected with control vector pRK5 **(A)** and full-length syndecan-3 cDNA **(B, C)**. 24 or 48 h post transfection, immunostaining with rabbit polyclonal anti-syndecan-3, followed by FITC-conjugated anti-rabbit antibody, was performed. Cells were analyzed by confocal microscopy. GFP fluorescence of COS-1 cells transfected with *GFPS3* (**D**) and *S3GFP* (**E, F**). The expression of syndecan-3 leads to the induction of long filopodia (arrows) and varicosities (arrowheads). Results are representative of at least four independent experiments. Bars represent 20 μm (A–E) and 3.3 μm (F). **(Panel B):** Schematic presentation of the vectors used in the transfection experiments. FL = full-length; GFP = green fluorescent protein. [Color figure can be viewed in the online issue, which is available at www.interscience.wiley.com.]

actin staining decreased with the distance from the cell body. Compared with the untransfected cells (Fig. 5B, E), in transfected cells the whole cytoskeleton was remodeled. Stress fibers disappeared and actin was re-distributed to the cell periphery, near the base and inside the filopodia-like structures, or re-organized into thick bundles (Fig. 5E). Scanning electron microscopy confirmed the immunocytochemical results in CHO K1 cells (Fig. 5G–I). As a result of transitory transfection, both the smooth untransfected and the hairy transfected phenotype with filopodia and microspikes were seen in the same cell preparations (Fig. 5G).

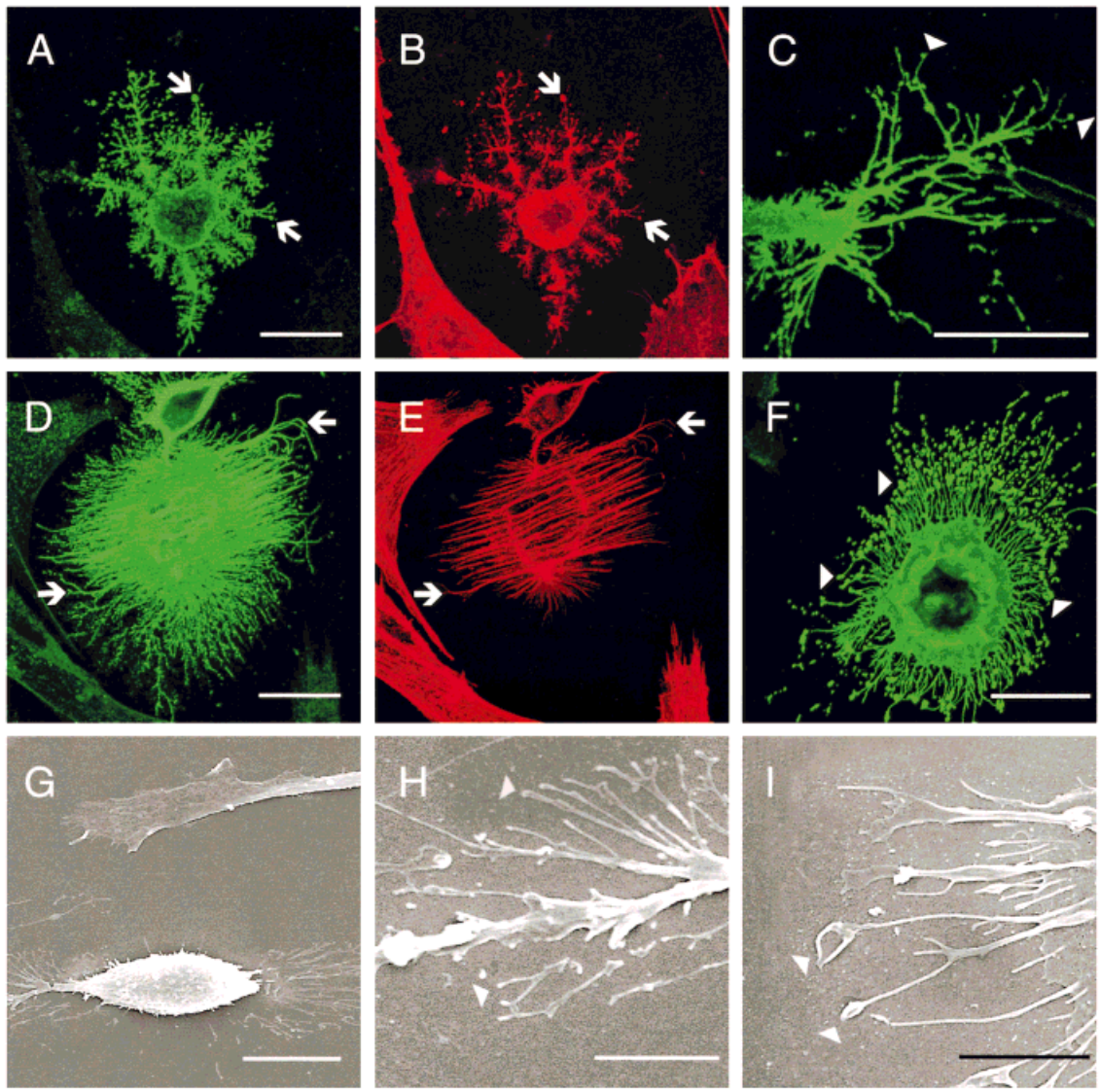

Fig. 5. Expression of syndecan-3 generates filopodia, microspikes and varicosities in 3T3 and CHO K1 cells. Liposome-mediated transfection of 3T3 SA (**A, B, C**) and CHO K1 (**D, E, F**) cells with the full-length syndecan-3. Immunocytochemistry with anti-syndecan-3 (A, C, D, F) antibody was performed as described in Figure 3. Actin was stained with TRITC-conjugated phalloidin (B, E). Arrowheads indicate varicosities. Syndecan-3 co-localizes with the actin cytoskeleton, especially in the cell periphery and the cell protrusions (arrows). Scanning electron microscopy was performed with CHO K1 cells (**G, H, I**), confirming the structural differences between transfected ''hairy'' and non-transfected cells (G). Detailed analysis (H, I) shows the fine structure of filopodia tips and varicosities (arrowheads). Results are representative of more than four (A–I) or two (G–I) independent experiments. Bars represent 20 μm (A–F), 10 μm (G), and 4 μm (H, I).

Figure 5H–I shows the detailed fine structure of filopodia tips and varicosities (Fig. 5H, I; arrowheads).

In order to find whether the effect obtained after syndecan-3 transfection might only be an artefact due to an abundance of syndecan-3 on the cell surface, we performed Laser Scanning Cytometry (LSC) analysis with transfected CHO K1 cells (data not shown). The results confirmed that the observed phenomenon were also caused by low expression of syndecan-3, and so were not an artifact due to great over-expression of the protein.

Importance of Glycosylation

In order to find whether the expression of the syndecan-3 core protein was sufficient to cause the phenotypes observed, or if the protein had to be glycosylated, CHO K1 (Fig. 6, Panel A: A, B) and CHO 745 cells (Fig. 6, Panel A: C, D) were

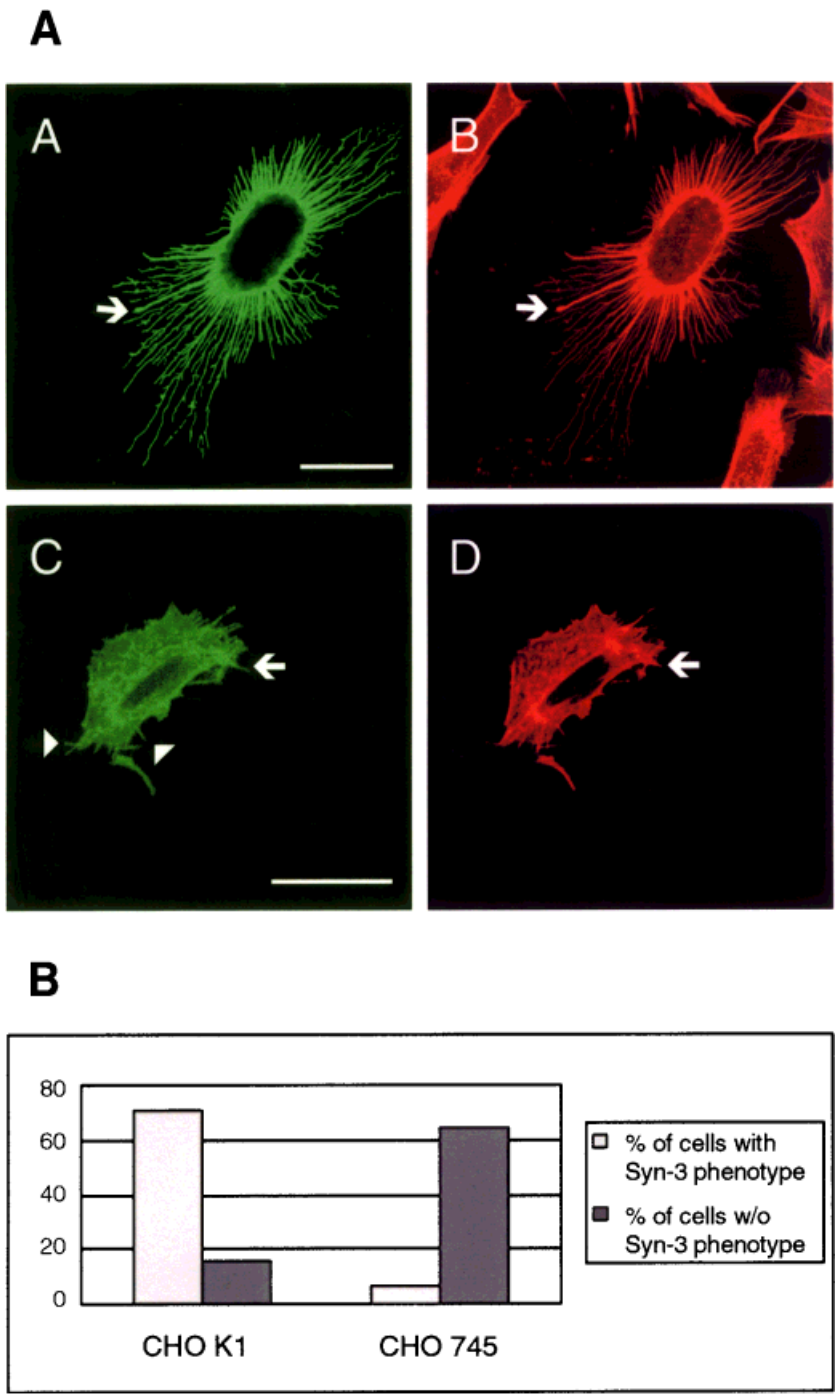

Fig. 6. The absence of sugar chains inhibits the formation of filopodia-like structures. **(Panel A):** Transfection and immunocytochemistry with anti-syndecan-3 (**A, C**) antibody was performed as described in Figure 3. Actin was stained with TRITC-conjugated phalloidin (**B, D**). In CHO K1 cells, the effect induced by full-length syndecan-3 was clearly seen (A) in the rearrangement of the actin cytoskeleton (B), which co-localized with the syndecan-3 protein (arrows). The majority of transfected CHO 745 cells (C, D) deficient in the production of the GAG-chains of the PG, only developed microspikes (arrowheads). Very few cells showed a syndecan-3 typical phenotype, although co-localization with actin could also be observed (arrows). Results are representative of three independent experiments. Bars: 20 μm. **(Panel B):** Transfected cells expressing the described phenotype, were quantified. About 700 CHO K1 cells and 150 CHO 745 cells were counted in three independent experiments. Results are expressed as percentage of cells showing an effect after transfection with full-length syndecan-3 DNA, in respect to the total transfected, syndecan-3 positive collective. The quantitative analysis proves the importance of sugar chains for the induction of the syndecan-3 phenotype. [Color figure can be viewed in the online issue, which is available at www.interscience.wiley.com.]

transfected and compared. The CHO 745 cell line is unable to synthesize GAG chains due to a defect in xylosyltransferase [Esko et al., 1985]. Most of the transfected CHO 745 cells showed membrane-staining and some microspikes on the cell-surface (Fig. 6, Panel A: C, D), but very few cells showed the phenotype as seen with CHO K1 (Fig. 6 Panel A: A, B). Only 8.7% of the transfected CHO 745 cells manifested a typical syndecan-3 phenotype, while 64.5% did not (Fig. 6, Panel B). In contrast, in the CHO-K1 cell line, 69.4% showed the typical syndecan-3 effects, while 12.7% did not show any difference from the wild type. Cells that were difficult to classify were omitted from the calculations (CHO K1: 17.9%; CHO 745: 26.8%).

To further determine the importance of the sugar chains, CHO K1 cells were transfected as before, then grown for 48 h in the absence and presence of 10 U/ml heparin. No cells bearing the syndecan-3 typical phenotype were seen in three independent experiments among the heparin-treated cells, while in the control the same amount of phenotype-presenting cells as in former experiments was observed. In the transfected CHO 745 and in the heparin-treated CHO K1 cells, a large number of cells (more than 30%) had a round form and retracted cell extensions as if they were in process of collapsing and de-attaching.

DISCUSSION

Human and Rodent Syndecan-3 are Highly Homologous

The sequence of the human syndecan-3 cDNA revealed an ORF of 1329 bp, predicting a polypeptide of 443 amino acids. High cDNA sequence and protein homology was found between the human syndecan-3 and that of other species like mouse, rat, and chicken. This high conservation of the syndecan-3 protein might reflect its biological importance in these organisms. Because of 100% homology in the transmembrane and cytoplasmic domain with the rodent protein, human syndecan-3 is assumed to have similar biochemical features, which are characteristic for these regions such as self-association [Asundi and Carey, 1995], tyrosine phosphorylation [Asundi and Carey, 1997] and serine phosphorylation by PKCβ [Prasthofer et al., 1995]. It might also interact via the last four amino acids of the C-terminal (EFYA) with proteins containing PDZ-domain [Zimmermann and David, 1999] such as syntenin [Grootjans et al., 1997] and CASK/LIN-2 [Hsueh and Sheng, 1999]. Proteins similar to syndesmos, which is a specific binding partner of syndecan-4 [Baciu et al., 2000], could also be seen as potential candidates for linking syndecan-3 to the cytoskeleton or for transferring syndecan-3-induced signals to intracellular pathways.

Although we found high homology in almost the entire sequence, surprisingly amino acids 7–23 were unique to the human protein. This region present in all clones screened was characterized by an accumulation of small, neutral amino acids (82%), comprising nine alanine and five glycine residues. Data bank comparison proved that an identical motif has not been described in other proteins so far. The highest similarity (72%) was found with the signal peptide from the fibroin protein [Tsujimoto and Suzuki, 1979]. The specific region lies in the putative signal peptide of the human syndecan-3 protein (amino acids 1–46), which was deduced from a hydrophobicity blot [Nielsen et al., 1997]. Although the signal peptides of the distinct species have different lengths (chicken: 22 amino acids [Gould et al., 1995] and rat: 45 amino acids [Carey et al., 1997b] and vary in their amino acid composition, the beginning (except for chicken) and the end are conserved. Therefore, we conclude that the human syndecan-3 signal peptide contains a human-specific sequence, which has no influence on the delivery of the protein to the plasma membrane.

Human Syndecan-3 mRNA is Highly Expressed in Brain, Adrenal Gland, and Spleen

The highest expression of syndecan-3 was found in the brain, adrenal gland, and spleen. The high expression detected in the whole nervous system (except for the pituitary gland) confirms the results of studies with rat N-syndecan [Carey et al., 1992; Carey, 1996]. Strong labeling was detected in the temporal lobe (highest signal), the corpus callosum, and the spinal cord. Accordingly, Hsueh and Sheng [1999] found high expression of rat syndecan-3 in the early post-embryonic brain, particularly in the cortex, corpus callosum, cerebellum, and thalamus. The high expression detected in the spinal cord and adrenal gland corroborates previous results [Nakanishi et al., 1997], while high expression of syndecan-3 in the spleen has

not been described. In the gastrointestinal system [Nakanishi et al., 1997], syndecan-3 mRNA was mainly found in the stomach, transverse colon, descending colon, duodenum, and rectum, while in the heart expression was predominantly seen in the aorta. As the syndecans are highly regulated, the expression pattern may depend on the stage of development. Nevertheless, in accord with the results from adult tissues, strong signals were also obtained in fetal brain and spleen, asserting the relevance of syndecan-3 function in these tissues. The only tumor cell line to show syndecan-3 expression was SW480. This might be due to the fact that the colon is one of the organs that expresses high levels of syndecan-3 mRNA. The lack of syndecan-3 mRNA detection in the other cell lines could mean either that they do not express detectable levels of syndecan-3 or that this expression was lost during transformation. For syndecan-1 it has been demonstrated that the loss of surface expression causes transformation of epithelial cells to mesenchyme-like cells, which are anchorage-independent [Kato et al., 1995].

Transient Transfection of Syndecan-3 Induces the Formation of Filopodia-Like Structures, Microspikes, and Varicosities

By focusing our interest on the expression of human syndecan-3 in transfected COS-1 cells, syndecan-3 was detected at the plasma membrane, where it co-localized with the actin cytoskeleton. While no morphological change was observed in control cells, the transfection of full-length syndecan-3 induced abundant filopodia-like structures (>5 μm), microspikes (<5 μm), and varicosities. Filopodia are cell elongations through which the cell receives and processes information about the environment, especially from the substrate. These structures are highly dynamic and can move the cell towards attracting signals [Mitchison and Cramer, 1996]. Comparably, the neuronal growth cone processes information about gradients of chemoattractants and chemorepellents and more- or less- adhesive substrata [Mackay et al., 1995; Mueller, 1999].

Sugar chains are required on the cell surface, since neither GAG-deficient CHO 745 cells nor heparin-treated CHO K1 cells developed the syndecan-3 typical phenotype on transfection. The small percentage of CHO 745 cells bearing the phenotype can be explained by a low remaining enzymatic activity (1/15) that is always present in the CHO 745 cell line [Esko et al., 1985]. According to our hypothesis, sugar-deficient syndecan-3 in CHO 745 cells would not bind cellular outgrowth promoting factors, which might be present in the medium. In treated CHO K1 cells, heparin would compete with the sugar chains of expressed syndecan-3. These findings show first the importance of sugar chains for the development of the syndecan-3 phenotype, and secondly suggest that a putative ligand would interact with syndecan-3 through its sugar residues.

Intracellular Pathways Responsible for Filopodia Formation are not Resolved

Since the filopodia-inducing effect of human syndecan-3 was observed in various cell types, such as COS-1, 3T3, and CHO K1 cells, a common intracellular signaling pathway may be involved. Some of the COS-1 cells also showed the syndecan-3 typical phenotype after transfection with *S3GFP*. This means, that the fusion of big tag such as GFP does not necessarily hinder the interactions between the cytoplasmic tail of syndecan-3 and intracellular proteins. This may be because the site of interaction is not (totally) masked, or the cytoplasmic domain has no important role in the outgrowth of filopodia. If this latter were the case, it would suggest a mechanism in which syndecan-3 after ligand binding becomes able to bind to other transmembrane proteins, which themselves would induce intracellular events. The study of stable cell lines expressing C-terminal deleted syndecan-3 will help to analyze this phenomenon further.

All processes lying downstream of ligand-binding to human syndecan-3 as receptor or co-receptor remain elusive. Nevertheless, the effect seen after syndecan-3 expression strongly resembles that observed after transfection experiments with syndecan-2, i.e., the formation of filopodia-like structures in COS-1 [Granés et al., 1999] and CHO K1 cells. The similarity of the phenotypes indicates that syndecan-3 transfection may also activate the cdc42 pathway. The involvement of small GTPases in the formation of specific actin cytoskeleton structures (such as microspikes, filopodia, lamellipodia, and stress fibers) is discussed elsewhere [Kozma et al., 1995; Tapon and Hall, 1997; Hall, 1998; Hu and Reichardt, 1999; Sander et al., 1999; Small et al., 1999].

Speculations can be made about the involvement of N-WASP (N-Wiskott-Adrich syndrome protein) and profilin downstream [Miki et al., 1998; Suetsugu et al., 1998] and about src/cortactin [Kinnunen et al., 1998], the ERM (Ezrin-Radixin-Moesin) family [Tsukita et al., 1997; Vaheri et al., 1997; Bretscher, 1999; Mangeat et al., 1999] and other PDZ proteins upstream of a putative cdc 42 activation. Nevertheless, further experiments are needed to get to know more about mechanisms.

Taken together, our results indicate that human syndecan-3 is similar to rodent syndecan-3 in cDNA and protein sequences and mRNA expression. Therefore, it is assumed to have similar biochemical features. The expression of human syndecan-3 leads to the induction of long, filopodia-like structures, microspikes, and varicosities and to the re-organization of the actin cytoskeleton. Its distribution in the induced prolongation suggests that syndecan-3 might interact with a ligand. In neurons, syndecan-3 is mainly found in axons, while syndecan-2 is concentrated in synapses, where it induces spine maturation [Hsueh et al., 1998; Ethell and Yamaguchi, 1999; Hsueh and Sheng, 1999]. Therefore we suggest that syndecan-3 may be involved in axon guidance in the nervous system in co-operation with syndecan-2 by controlling cell outgrowth and migration.

ACKNOWLEDGMENTS

We thank Ana Marcos, Manuel Rivas, Susana Castel, and Alex Monna for their excellent technical assistance, Roser Pagan and Myriam Fabre for fruitful comments on the manuscript and Dr. Bernfield for the kind gift of the plasmid pMB284 and the anti-syndecan-3 antibody.

REFERENCES

Asundi VK, Carey DJ. 1995. Self-association of N-syndecan (syndecan-3) core protein is mediated by a novel structural motif in the transmembrane domain and ectodomain flanking region. J Biol Chem 270(44):26404–26410.

Asundi VK, Carey DJ. 1997. Phosphorylation of recombinant N-syndecan (syndecan-3) core protein. Biochem Biophys Res Commun 240:502–506.

Baciu PC, Saoncella S, Lee SH, Denhez F, Leuthardt D, Goetinck PF. 2000. Syndesmos, a protein that interacts with the cytoplasmic domain of syndecan-4, mediates cell spreading and actin cytoskeletal organization. J Cell Sci 113:315–324.

Bernfield M, Kokenyesi R, Kato M, Hinkes MT, Spring J, Gallo RL, Lose EJ. 1992. Biology of the syndecans: a family of transmembrane heparan sulfate proteoglycans. Annu Rev Cell Biol 8:365–393.

Bretscher A. 1999. Regulation of cortical structure by the ezrin-radixin-moesin protein family. Curr Opin Cell Biol 11:109–116.

Carey DJ. 1996. N-Syndecan: structure and function of a transmembrane heparan sulfate proteoglycan. Perspect Dev Neurobiol 3:331–346.

Carey DJ. 1997a. Syndecans: multifunctional cell-surface co-receptors. Biochem J 327:1–16.

Carey DJ, Evans DM, Stahl RC, Asundi VK, Conner KJ, Garbes P, Cizmeci-Smith G. 1992. Molecular cloning and characterization of N-syndecan, a novel transmembrane heparan sulfate proteoglycan. J Cell Biol 117(1):191–201.

Carey DJ, Conner K, Asundi VK, O'Mahony DJ, Stahl RC, Showalter L, Cizmeci-Smith G, Hartman J, Rothblum LI. 1997b. cDNA cloning, genomic organization and in vivo expression of rat N-syndecan. J Biol Chem 272(5):2873–2879.

Chernousov MA, Carey DJ. 1993. N-syndecan (syndecan-3) from neonatal rat brains binds basic fibroblast growth factor. J Biol Chem 268(22):16810–16814.

Chernousov MA, Stahl RC, Carey DJ. 1996. Schwann cells secrete a novel collagen-like adhesive protein that binds N-syndecan. J Biol Chem 271:13844–12853

Esko JD, Stewart TE, Taylor WH. 1985. Animal cell mutants defective in glycosaminoglycan biosynthesis. Proc Natl Acad Sci 82:3197–3201.

Ethell IM, Yamaguchi Y. 1999. Cell surface heparan sulfate proteoglycan syndecan-2 induces the maturation of dendritic spines in rat hippocampal neurons. J Cell Biol 144(3):575–586.

Fuentealba L, Carey DJ, Brandan E. 1999. Antisense inhibition of syndecan-3 expression during skeletal muscle differentiation accelerates myogenesis through a basic fibroblast growth factor-dependent mechanism. J Biol Chem 274(53):37876–37884.

Gould SE, Upholt WB, Kosher RA. 1992. Syndecan-3: a member of the syndecan family of transmembrane-intercalated proteoglycans that is expressed in high amounts at the onset of chicken limb cartilage differentiation. Proc Natl Acad Sci USA 89:3271–3275.

Gould SE, Upholt WB, Kosher RA. 1995. Characterization of chicken syndecan-3 as a heparan sulfate proteoglycan and its expression during embryogenesis. Dev Biol 168(2):438–451.

Granés F, García R, Casaroli-Marano RP, Castel S, Rocamora N, Reina M, Ureña J, Vilaró S. 1999. Syndecan-2 induces filopodia by active cdc42Hs. Exp Cell Res 248:439–456.

Grootjans JJ, Zimmermann P, Reekmans G, Smets A, Degeest G, Dürr J, David G. 1997. Syntenin, a PDZ protein that binds syndecan cytoplasmic domains. Proc Natl Acad Sci USA 94:13683–13688.

Hall A. 1998. Rho GTPases and the actin cytoskeleton. Science 279:509–513.

Howe A, Aplin AE, Alahari SK, Juliano RL. 1998. Integrin signaling and cell growth control. Curr Opin Cell Biol 10(2):220–231.

Hsueh YP, Sheng M. 1999. Regulated expression and subcellular localization of syndecan heparan sulfate proteoglycans and the syndecan-binding protein CASK/LIN-2 during rat brain development. J Neurosci 19(17):7415–7425.

Hsueh YP, Yang FC, Kharazia V, Naisbitt S, Cohen AR, Weinberg RJ, Sheng M. 1998. Direct interaction of CASK/LIN-2 and syndecan heparan sulfate proteoglycan and their overlapping distribution in neuronal synapses. J Cell Biol 142(1):139–151.

Hu S, Reichardt LF. 1999. From the membrane to cytoskeleton: enabling a connection. Neuron 22:419–422.

Kato M, Saunders S, Nguyen H, Bernfield M. 1995. Loss of cell surface syndecan-1 causes epithelia to transform into anchorage-independent mesenchyme-like cells. Mol Biol Cell 6:559–576.

Kim CW, Goldberger RL, Gallo RL, Bernfield M. 1994. Members of the syndecan family of heparan sulfate proteoglycans are expressed in distinct cell-, tissue-, and development-specific patterns. Mol Biol Cell 5(7):797–805.

Kinnunen T, Raulo E, Nolo R, Maccarana M, Lindahl U, Rauvala H. 1996. Neurite outgrowth in brain neurons induced by heparin-binding growth-associated molecule (HB-GAM) depends on the specific interaction of HB-GAM with heparan sulfate at the cell surface. J Biol Chem 271(4):2243–2248.

Kinnunen T, Kaksonen M, Saarinen J, Kalkkinen N, Peng HB, Rauvala H. 1998. Cortactin-Src kinase signaling pathway is involved in N-syndecan dependent neurite outgrowth. J Biol Chem 273(17):10702–10708.

Kozma R, Ahmed S, Best A, Lim L. 1995. The Ras-related protein Cdc42Hs and bradykinin promote formation of peripheral actin microspikes and filopodia in Swiss 3T3 fibroblasts. Mol Cell Biol 15(4):1942–1952.

Lauri SE, Rauvala H, Kaila K, Taira T. 1998. Effect of heparin-binding growth-associated molecule (HB-GAM) on synaptic transmission and early LTP in rat hippocampal slices. Eur J Neurosci 10:188–194.

Lauri SE, Kaukinen S, Kinnunen T, Ylinen A, Imai S, Kaila K, Taira T, Rauvala H. 1999. Regulatory role and molecular interactions of a cell-surface heparan sulfate proteoglycan (N-syndecan) in hippocampal long-term potentiation. J Neurosci 19(4):1226–1235.

Mackay DJG, Nobes CD, Hall A. 1995. The Rho's progress: a potential role during neuritogenesis for the Rho family of GTPases. TINS 18(11):496–501.

Mangeat P, Roy C, Martin M. 1999. ERM proteins in cell adhesion and membrane dynamics. Trends Cell Biol 9:187–192.

Miki H, Sasaki T, Takai Y, Takenawa T. 1998. Induction of filopodium formation by a WASP-related actin-depolymerizing protein N-WASP. Nature 391(6662):93–96.

Mitchison TJ, Cramer LP. 1996. Actin-based cell motility and cell locomotion. Cell 84:371–379.

Mueller BK. 1999. Growth cone guidance: first steps into a deeper understanding. Annu Rev Neurosci 22:351–388.

Nakanishi T, Kadomatsu K, Okamoto T, Ichihara-Tanaka K, Kojima T, Saito H, Tomoda Y, Muramatsu T. 1997. Expression of syndecan-1 and -3 during embryogenesis of the central nervous system in relation to binding with midkine. J Biochem 121(2):197–205.

Nielsen H, Engelbrecht J, Brunak S, von Heijne G. 1997. Identification of prokaryotic and eukaryotic signal peptides and prediction of their cleavage sites. Protein Eng 10:1–6.

Nolo R, Kaksonen M, Raulo E, Rauvala H. 1995. Co-expression of heparin-binding growth-associated molecule (HB-GAM) and N-syndecan (syndecan-3) in developing rat brain. Neurosci Lett 191:39–42.

Prasthofer T, Ek B, Ekman P, Owens R, Hook M, Johansson S. 1995. Protein kinase C phophorylates two of the four known syndecan cytoplasmic domains in vitro. Biochem Mol Biol Int 36(4):793–802.

Raulo E, Chernousov MA, Carey DJ, Nolo R, Rauvala H. 1994. Isolation of a neuronal cell surface receptor of heparin binding growth-associated molecule (HB-GAM). J Biol Chem 269(17):12999–13004.

Sander EE, ten Klooster JP, van Delft S, van der Kammen RA, Collard JG. 1999. Rac downregulates Rho activity: reciprocal balance between both GTPases determines cellular morphology and migratory behavior. J Cell Biol 147(5):1009–1021.

Small JV, Rottner K, Kaverina I. 1999. Functional design in the actin cytoskeleton. Curr Opin Cell Biol 11:54–60.

Suetsugu S, Miki H, Takenawa T. 1998. The essential role of profilin in the assembly of actin for microspike formation. EMBO J 17:6516–6526.

Takeichi M. 1991. Cadherin cell adhesion receptors as a morphogenetic regulator. Science 251(5000):1451–1455.

Tapon N, Hall A. 1997. Rho, rac and cdc42 GTPases regulate the organization of the actin cytoskeleton. Curr Opin Cell Biol 9:86–92.

Tsujimoto Y, Suzuki Y. 1979. Structural analysis of the fibroin gene at the 5′ end and its surrounding regions. Cell 16(2):425–436.

Tsukita S, Yonemura S, Tsukita S. 1997. ERM (ezrin/radixin/moesin) family: from cytoskeleton to signal transduction. Curr Opin Cell Biol 9:70–75.

Vaheri A, Carpen O, Heiska L, Helander TS, Jaaskelainen J, Majander-Nordenswan P, Sainio M, Timonen T, Turunen O. 1997. The ezrin protein family: membrane-cytoskeleton interactions and disease associations. Curr Opin Cell Biol 9(5):659–666.

Woods A, Couchman JR. 1998. Syndecans: synergistic activators of cell adhesion. Trends Cell Biol 8:189–192.

Zimmermann P, David G. 1999. The syndecans, tuners of transmembrane signaling. FASEB J 13:91–100.